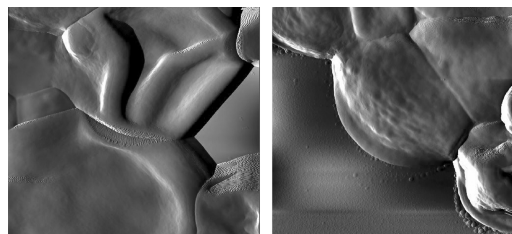


Truly Nonionic Polymer Shells for the Encapsulation of Living Cells

Jessica L. Carter,^a Irina Drachuk,^a Svetlana Harbaugh,
Nancy Kelley-Loughnane, Morley Stone, Vladimir V. Tsukruk*

Engineering surfaces of living cells with natural or synthetic compounds can mediate intercellular communication and provide a protective barrier from hostile agents. We report on *truly nonionic* hydrogen-bonded LbL coatings for cell surface engineering. These ultrathin, highly permeable polymer membranes are constructed on living cells without the cationic component typically employed to increase the stability of LbL coatings. Without the cytotoxic cationic PEI pre-layer, the viability of encapsulated cells drastically increases to 94%, in contrast to 20% viability in electrostatically-bonded LbL shells. Moreover, the long-term growth of encapsulated cells is not affected, thus facilitating efficient function of protected cells in hostile environment.



Bare Cells

Encapsulated Cells

Introduction

Cells encapsulated in synthetic media show great potential for biomedical applications, including biomimetics, biosensing, enhancing biocompatibility of implantable materials, and may represent an important step toward construction of an artificial cell.^[1–3] Engineering surfaces of living cells with natural or synthetic compounds can mediate intercellular communication, render the cells less sensitive to harsh environmental changes, and provide a protective barrier from hostile agents.^[4–6] Encapsulation of living cells has been demonstrated through use of sol/gel reaction and crosslinked hydrogels.^[7,8] However, sol/gels are typically formed by hydrolysis and condensation of tetraethyl/

methyl orthosilicates. This method produces ethanol/methanol, which is deleterious to cell encapsulation as these byproducts are damaging to cells.^[9,10] pH-neutral sol/gel encapsulation has been demonstrated to yield cells with higher enzymatic activity than the traditional method, but still lower activity than non-encapsulated cells.^[11] Thus, naturally derived and therefore biocompatible hydrogels, such as alginate, have been utilized. Alginate is a natural, nonmammalian polysaccharide that forms a gel in the presence of divalent cations via ionic crosslinking. Because alginate does not naturally promote cell interactions,^[12,13] the alginate has been modified through the addition of RGD, a cell adhesion oligopeptide.^[10,14] A critical advantage to alginate is its gentle gelling behavior, which allows encapsulation of cells with minimal trauma.^[15,16] Disadvantages of this material is that it is not naturally broken down enzymatically in mammals and, hence, has poorly regulated degradation.^[17]

Layer-by-layer (LbL) assembly is a popular fabrication method for charged macromolecules and particles introduced in 1990 s.^[18–30] This assembly is considered a simple and reliable method for forming permeable, nanoporous shells from cationic and anionic polymers.^[31–34] Freely-

J. L. Carter, I. Drachuk, Vladimir V. Tsukruk
School of Materials Science and Engineering, Georgia Institute of
Technology, Atlanta, GA 30332, USA
E-mail: vladimir@mse.gatech.edu
S. Harbaugh, N. Kelley-Loughnane, M. Stone
Air Force Research Laboratory, Directorate of Human
Effectiveness, Wright-Patterson AFB, Dayton, OH 45433, USA

*J. L. Carter and I. Drachuk contributed equally to this work.

standing LbL structures with controlled physical properties have been introduced in our group.^[35–40] Conformal coating of geometrically diverse templates, a precise control of the membrane thickness, and the ability to tune the membrane functionalities and properties are among the main advantages of the LbL approach which can be utilized for formation of hollow microcapsules and ultrathin shells for cells.^[41–48] The ability to tailor membrane permeability is of particular importance for encapsulation of living cells, as cell viability critically depends on the diffusion of nutrients through the artificial polymer membrane.

A wide variety of cell types which have successfully been encapsulated using LbL assembly include stem cells, bacteria, bacteria spores, pancreatic islets, and platelets.^[49–54] The use of synthetic polycations in conventional LbL assembly, such as poly(styrene sulfonate) (PSS), poly(allylamine hydrochloride) (PAH), and polyethylenimine (PEI) pose severe limitations on the potential application of the LbL approach to cell surface engineering. It has been suggested that overall toxicity of the polyelectrolytes originates from the positive charge of polycations. This charge results in permeabilization of the cell membrane, causing its damage and, eventually, cell death.^[55,56] The use of natural polymers, such as poly(L-lysine) (PLL), a polypeptide, and hyaluronic acid (HA), a polysaccharide, allow for encapsulation with reduced deleterious effects of cell proliferation.^[57] Nonelectrostatically assembled LbL films are considered to be promising for designing structures on biological systems.^[58–60]

In order to design individual cell-compatible synthetic shells, we recently designed highly permeable, hydrogen-bonded LbL coatings utilizing tannic acid (TA), and poly(*N*-vinylpyrrolidone) (PVPON), which result in coatings responsive under biologically and physiologically relevant conditions that are suitable for engineering cell surfaces while increasing cell viability.^[61–65] In TA/PVPON systems, cell viability following encapsulation was increased to 79%, as opposed to merely 20% in conventional PSS/PAH systems. However, in the application of the LbL technique to cell surfaces, a precursor layer such as PEI was utilized to provide enhanced adhesion of the subsequent multilayers.^[66–68] This allows the use of PEI as an almost universal priming layer that eliminates many of the uncertainties associated with a poorly defined surface charge. However, the cytotoxicity of PEI component might have a negative effect on cell function.^[69] Consequently, the development of an encapsulation LbL method that would increase cell viability without sacrificing the desired diffusion properties and mechanical stability of the shells is highly desirable.

Therefore, we introduce *truly nonionic* hydrogen-bonded LbL coatings for cell surface engineering capable of long-term support of cell function and conducted comprehensive monitoring of cell viability directly after LbL assembly and

continuously across all stages of the cell growth. In this study, we show that ultrathin, permeable hydrogen-bonded shells can be constructed on living cells without a cationic pre-layer, facilitating significantly increased viability of encapsulated cells which reaches 94%. *Saccharomyces cerevisiae* yeast cells employed here, a well-known cell type which is considered a good model of eukaryotic cells because of its completely sequenced genome, is used in this study.^[70] *S. cerevisiae* yeast cells with incorporated green fluorescent protein (GFP) reporters have been used for enzyme and protein analysis.^[71–73]

Experimental Section

Materials

TA ($\bar{M}_w = 1700$ Da), PVPON of two molecular weights ($\bar{M}_w = 360\,000$ and $130\,000$ Da), branched PEI ($\bar{M}_w = 25\,000$ Da), mono- and dibasic sodium phosphate, poly-*N*-vinylpyrrolidone (PVPON), galactose, and glucose were purchased from Sigma-Aldrich. Alexa Fluor 532 carboxylic acid succinimidyl ester fluorescent dye was purchased from Invitrogen. To visualize the polyelectrolyte membrane in confocal laser scanning microscopy (CLSM), Alexa Fluor 532-PVPON was used during the deposition of the outermost (TA/PVPON) bilayer. Alexa Fluor 532-PVPON was synthesized according to the established procedure.^[39] All solutions were filter-sterilized with polystyrene nonpyrogenic membrane systems (0.22 μm pore size, Corning filter system) before applying to the cells. Ultrapure (Nanopure system) filtered water with a resistivity of $18.2\ \text{M}\Omega \cdot \text{cm}$ was used for experiments.

The *S. cerevisiae* YPH501 diploid yeast strain expressing yEGFP (yeast-enhanced GFP) were used for this study.^[39] Cells were cultured in synthetic minimal medium (SMM) supplemented with appropriate dropout solution and sugar source, 2% glucose. Yeast cells were grown at $30\ ^\circ\text{C}$ in a shaker incubator (New Brunswick Scientific) with 225 rpm to bring them to an early exponential phase [with optical density at 600 nm (OD₆₀₀ test) = 0.3–0.4].

Encapsulation of Cells with Nonionic Hydrogen-Bonded Shells

LbL assembly was employed for encapsulation of individual yeast cells with nonionic hydrogen-bonded multilayers of TA/PVPON as described in detail in previous publication (Figure 1).^[39] For comparison, we also performed encapsulation of yeast cells with PEI-primed layer ($0.5\ \text{mg} \cdot \text{mL}^{-1}$ in $0.1\ \text{M}$ NaCl, pH = 7) followed by consecutive deposition of TA and PVPON. Before deposition of the (TA/PVPON)_{*n*} LbL shells (where *n* denotes the number of deposited bilayers) yeast cells were harvested in 1.5 mL microcentrifuge tubes by centrifugation at 4 000 rpm for 2 min and washed three times in phosphate buffer ($0.01\ \text{M}$ in $0.1\ \text{M}$ NaCl, pH = 6). Layers of TA and PVPON were allowed to adsorb onto yeast cell membrane from 0.5 and $2\ \text{mg} \cdot \text{mL}^{-1}$ aqueous solution ($0.01\ \text{M}$ phosphate buffer and $0.1\ \text{M}$ NaCl at pH = 6) for 15 min. During LbL deposition, cells were re-dispersed in the appropriate solution by gentle shaking (at 225 rpm). After deposition of each layer, cells were collected in a

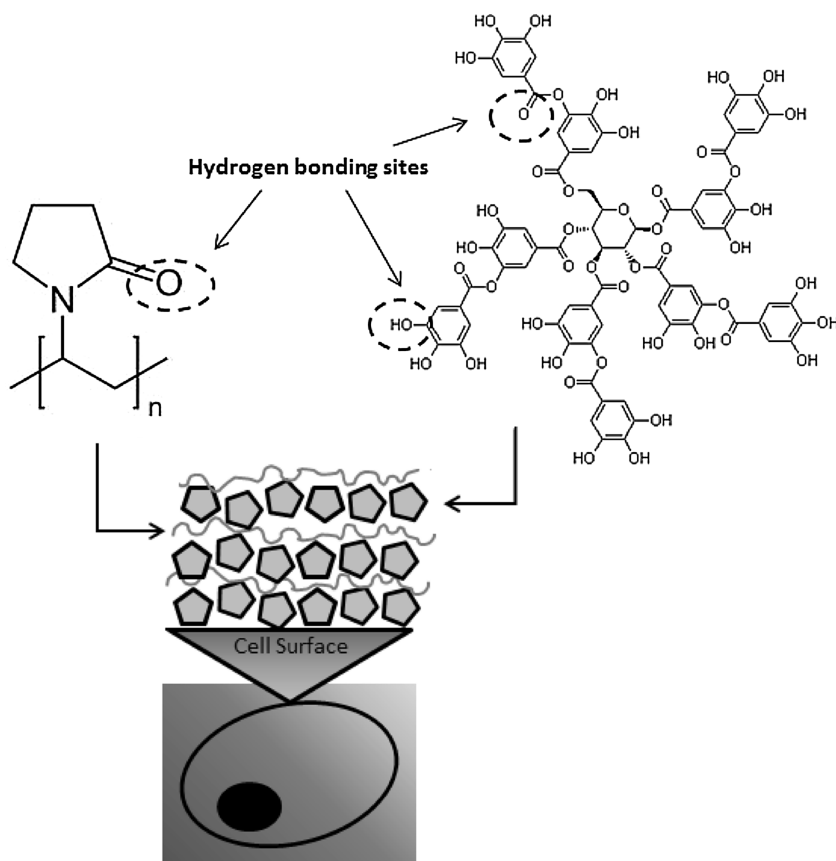


Figure 1. Schematic illustrating the formation of hydrogen-bonded TA/PVPON shell on yeast cell surfaces.

pellet by centrifugation and washed three times with phosphate buffer.

CLSM

Encapsulated cells were incubated in 2% raffinose and 2% galactose in SMM yeast media at 30 °C to induce the yEGFP production. Optical density at 600 nm and yEGFP fluorescence at 513 nm were measured at indicated time points. Confocal images of encapsulated and non-encapsulated yeast cells were obtained with an LSM 510 NLO META inverted confocal microscope equipped with 63 × 1.4 oil immersion objective lens (Zeiss).

ζ-Potential

Independent measurements of ζ-potentials on encapsulated yeast cells after deposition of each layer were performed on Zetasizer Nano-ZS equipment (Malvern). Yeast cells were collected at mid-log phase (OD = 0.6–0.8), washed three times in a solution of 0.01 M phosphate buffer and 0.1 M NaCl at pH = 6.0 before depositing subsequent layers of TA and PVPON ($M_w = 360$ kDa). After deposition and washing, 100 mL of encapsulated cells were combined with 900 mL of deionized nanopure water to obtain 1 mL of solution to perform ζ-potential measurements. Each value was acquired by averaging three independent measurements of 40 sub-runs each.

Atomic Force Microscopy (AFM)

Surface topography and roughness of bare and encapsulated yeast cells was examined using AFM. Cells were washed, deposited onto a solid substrate, and allowed to dry before scanning. Thickness of collapsed hollow polymer capsules was also measured using AFM. AFM images were collected using a Dimension-3000 (Digital Instruments) microscope in the “light” tapping mode according to the well-established procedure.^[74,75]

Fluorescence Recovery after Photobleaching (FRAP)

Experiments on permeability were performed using CLSM with photobleaching of fluorescein isothiocyanate (FITC) fluorescent molecules inside the capsule. We used the well-known standard procedure for estimating permeability properties using FRAP technique which has been also applied to LbL microcapsules.^[76–78] In this technique, polymeric hollow microcapsules serve as model system to evaluate and compare permissive properties as a function of shell structure. Since basic nutrients (glucose, essential amino acids) and inducer molecules (e.g., galactose, $M_w = 180$ Da) are comparable in size with FITC molecules ($M_w = 380$ Da), we suggest that these molecules will also be able to freely pass through the shell membrane and be available for proper cell function.

Hollow capsules of hydrogen-bonded TA/PVPON with 4, 5, and 6 bilayers were prepared on silica microparticles with a diameter similar to the cell dimensions and slightly negatively charged surface followed by core dissolution as described earlier.^[79] 100 mL of hollow capsules solution was combined with 200 mL of 1 mg · mL⁻¹ FITC solution (pH = 6) and allowed to settle down in a Lab-Tek chamber glass cell for 3 h. A laser beam (488 nm) was focused within a region of interest (ROI) inside a capsule, and pulsed at 100% intensity to photobleach the dye molecules. Each experiment started with three pre-bleached image scans followed by 25–35 bleach pulse exposures of 3 ms each within ROI. The bleaching time was adjusted to ensure complete photobleaching of FITC inside the capsule. The fluorescence recovery was monitored by capturing 30 scans of 3 ms exposure at 3% laser intensity. The recovery was considered complete when the intensity of the photobleached region stabilized. The quantitative analysis was performed using *ImageJ* software, and curve-fitting, as described in detail elsewhere.^[39]

Resazurin Assay

Cell viability was measured using a resazurin assay.^[80,81] Control (non-treated) and encapsulated cells were re-suspended in 1 mL of media. 100 mL of resazurin (7-hydroxy-3H-phenoxazin-3-one 10-oxide) solution was added to cell cultures. The mixtures were incubated at 30 °C for 2 h. Fluorescence intensity was measured at $\lambda = 590$ nm ($\lambda_{ex} = 560$ nm).

Results and Discussion

Morphology of LbL Shells

The main hypothesis of this study was that the application of true hydrogen-bonded shells for cell encapsulation and elimination of polycationic components which are usually presented in LbL shells can potentially dramatically increase cell viability without effecting cell function. Therefore, in this study we utilized the ability of TA to precipitate proteins (and hence form tight adhesions with the cell surface) to create hydrogen bonding with neutral polymers around cell surfaces without utilization of cationic pre-layer as has been exploited in our earlier study to stabilize LbL assembly.^[79] Association of TA with various neutral and charged synthetic polymers has been extensively explored by the Sukhishvili group for the fabrication of hydrogen-bonded LbL films.^[62] Particularly they showed that for PVPON/TA system below $\text{pH} < 7.5$ (for $\text{pK}_a = 8.5$), phenolic hydroxyl groups of TA form multiple hydrogen bonds with carbonyl groups of pyrrolidone rings due to multiple hydrogen donor sites available in one TA molecule thus facilitating LbL assembly (Figure 1).

LbL shells of $(\text{TA}/\text{PVPON})_n$ were formed around the YPH501 cells. Hydrogen bonding between the hydroxyl groups of TA and the carbonyl groups of PVPON preserve cell integrity and function under deposition conditions.^[54,82–84] The successful formation of shells around cells was confirmed by confocal microscopy (Figure 2). Figure 2a demonstrates large scale confocal image of encapsulated yeast cells with fluorescently labeled PVPON (PVPON-co-Alexa Fluor 532) and Figure 2b shows the same area in transmission optical mode, confirming that *all the cells* visible in the selected area have been uniformly coated with labeled LbL shells.

We perform AFM imaging to visualize the surface morphology of coated cell surfaces and evaluate the initial

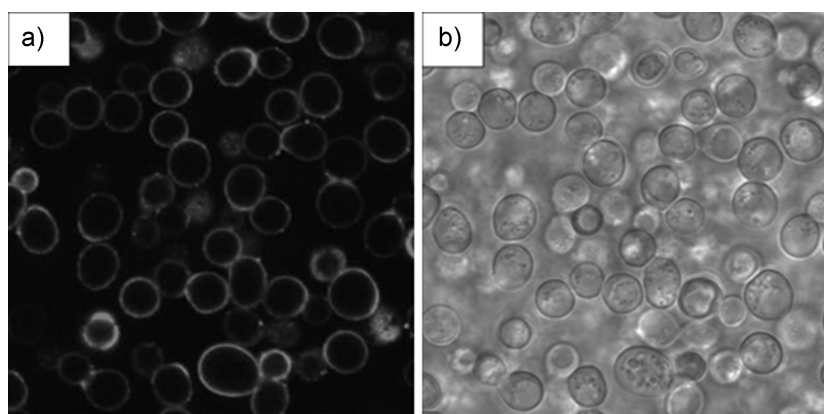


Figure 2. CLSM images of $(\text{TA}/\text{PVPON})_4$ coated cells. (a) Large scale confocal image of encapsulated yeast cells with fluorescently labeled PVPON-co-Alexa Fluor 532. (b) The same area in transmission mode.

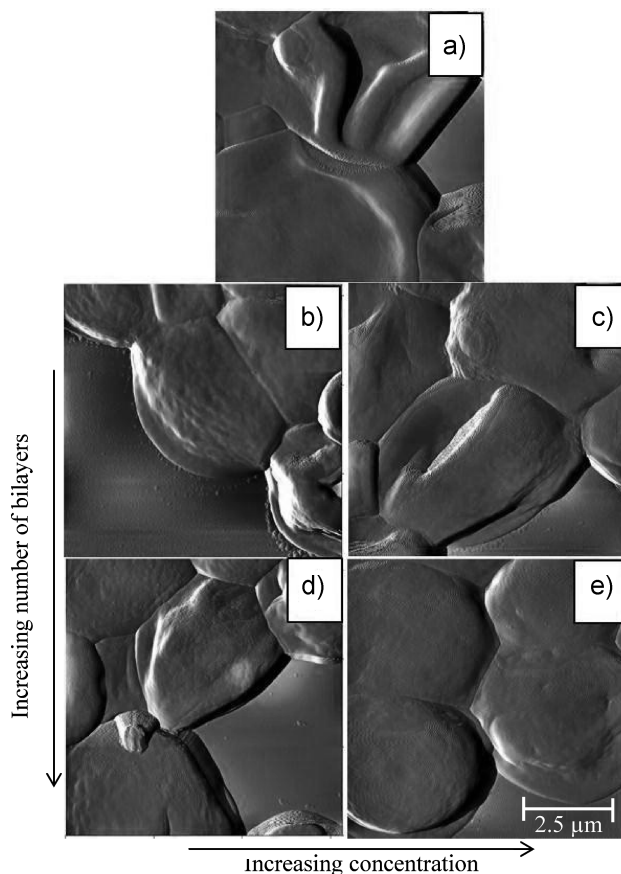


Figure 3. AFM amplitude images of (a) bare and (b)–(e) coated YPH501 yeast cells. Concentrations refer to TA & PVPON solutions. (b) 1 bilayer, $0.5 \text{ mg} \cdot \text{mL}^{-1}$; (c) 1 bilayer, $2 \text{ mg} \cdot \text{mL}^{-1}$; (d) 2 bilayers, $0.5 \text{ mg} \cdot \text{mL}^{-1}$; (e) 2 bilayers, $2 \text{ mg} \cdot \text{mL}^{-1}$.

microroughness and subsequent smoothing of cell surfaces (Figure 3). AFM topographical images showed overall round shape and microscopic dimensions of cells as well as fine surface features for (a) bare, single bilayer (estimated thickness of 3.4 nm) with polymer concentrations of (b) 0.5 and (c) $2 \text{ mg} \cdot \text{mL}^{-1}$, and two bilayers (estimated thickness of 6.8 nm) with concentrations of (d) 0.5 and (e) $2 \text{ mg} \cdot \text{mL}^{-1}$. 3D renderings of these coated cells at higher magnification are shown in Figure 4.

Overall, AFM images collected here showed that encapsulation of cells with the first bilayer increases the microroughness of the cell surface at small surface areas. However, following bilayer addition as well as increasing concentration of solution both result in smoothing of the cell surface as was confirmed with microroughness measurements. For this purpose, the average root mean square

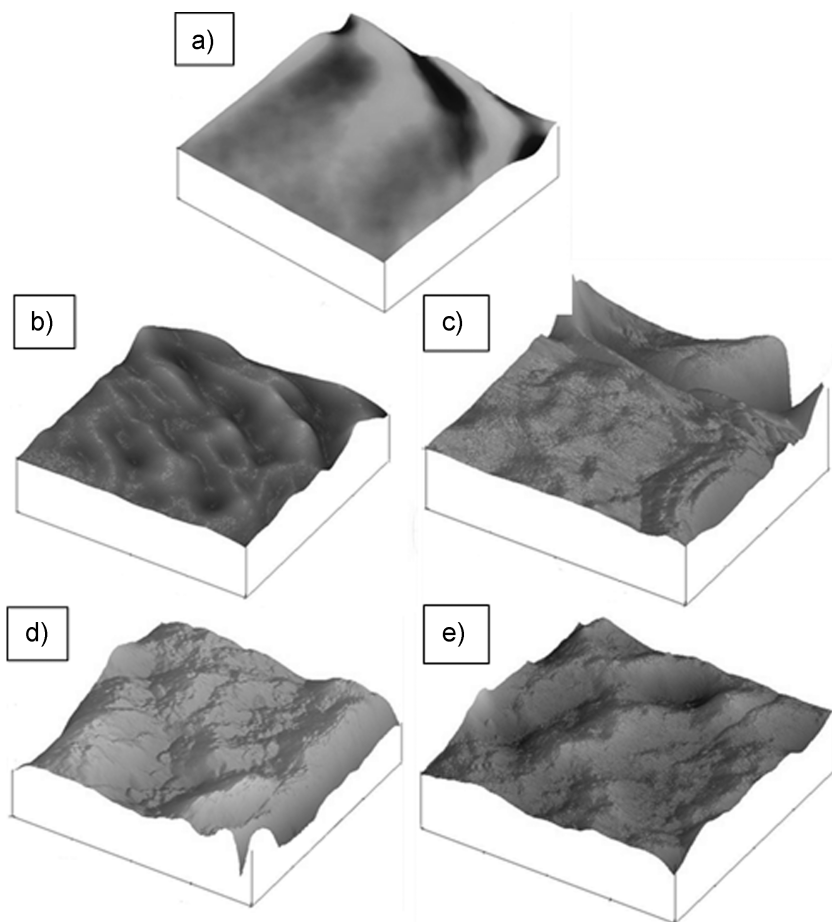


Figure 4. 3D topographical AFM images of (a) bare and (b)–(e) coated YPH501 yeast cells. Concentrations refer to TA & PVPON solutions. Scale is $2 \times 2 \mu\text{m}^2$, Z-scale is 20 nm. (b) 1 bilayer, $0.5 \text{ mg} \cdot \text{mL}^{-1}$; (c) 1 bilayer, $2 \text{ mg} \cdot \text{mL}^{-1}$; (d) 2 bilayers, $0.5 \text{ mg} \cdot \text{mL}^{-1}$; (e) 2 bilayers, $2 \text{ mg} \cdot \text{mL}^{-1}$.

(RMS) roughness was taken from a $100 \text{ nm} \times 100 \text{ nm}^2$ surface area on AFM scans for various encapsulated cells (Figure 5). As was observed, initial modest microroughness of 4 nm for bare cell surface increases more than twofold, to 9 nm, after coating with a single bilayer but decreases slightly for two bilayer coating. Also, if LbL coatings have been deposited from higher concentration solution, the overall microroughness remains close to that for the bare cell surface (around 3.5 nm). The resulting smoothed surface is evidence that uniform, conformal, and homogeneous LbL coatings can be deposited on the cells if more than two bilayers are deposited from higher solution concentration.

As z-potential studies demonstrated, the absence of cationic pre-layer during LbL assembly caused little changes in the surface charge of the cells in contrast to previous studies with PEI pre-layer which resulted in sharp change to positive values (Figure 6).^[61] Maintaining constant and high ζ -potential on cell surfaces results in good cell

suspension stability and prevents common aggregation of cells during LbL assembly, which further simplifies the formation of uniform cell layers and study of their viability.^[46] The ζ -potential remains nearly constant (around -50 mV). During deposition of hydrogen-bonded components among carboxylic groups of TA and carbonyl groups of neutral polymer (PVPON) at $\text{pH} = 6.0$, the net surface charge remained negative, and the ζ -potential oscillated between negative values with a standard deviation of $\sim 5 \text{ mV}$. Small oscillation of ζ -potential can be attributed to a lower amount of the neutral polymer deposited during LbL assembly.^[44] Therefore, the lower the thickness of PVPON and the stronger the intermolecular hydrogen-bonded interactions between TA and PVPON the more pronounced effect of TA as a negatively-charged weak polyelectrolyte on the overall surface charge potential.

Viability and Growth of Encapsulated Cells with Different Shell Morphologies

The viability of encapsulated cells was assessed with the resazurin assay as was discussed elsewhere.^[53,54] Bioreduction of resazurin is achieved by reducing enzyme cofactors in viable cells and results in the conversion of resazurin's oxidized blue form to its pink fluorescent intermediate, resorufin.^[85] The absence of such cofactors in dead cells leads to no conversion and no fluorescence can be detected.^[86]

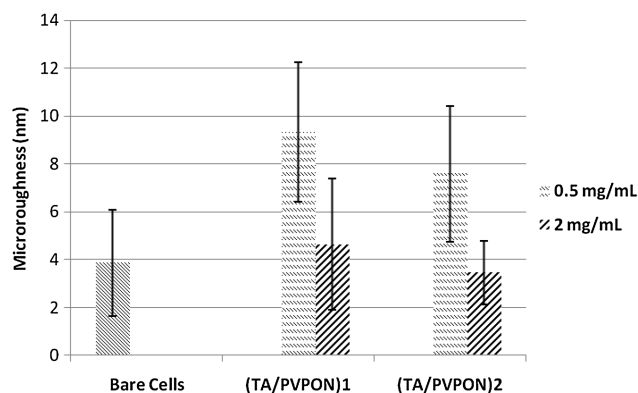


Figure 5. Microroughness for cell surfaces without shell and with different shells.

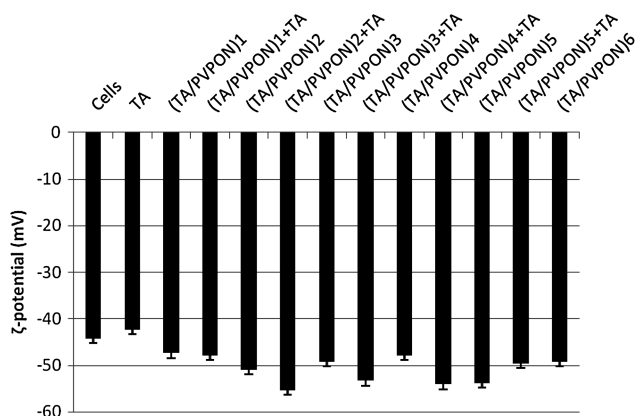


Figure 6. ζ -Potential of bare and encapsulated cells with different shells at pH = 6.

Figure 7 shows viability of cells encapsulated with truly nonionic LbL shells in comparison with the same cells encapsulated but with cationic PEI pre-layer as a control series explored in previous study with different PVPON molecular weight.^[61] In this study, different molecular weights of PVPON (360 or 1 300 kDa) and different numbers of TA/PVPON bilayers (two or four) have been explored. As apparent from these results, cells coated with fully nonionic (TA/PVPON) shell showed higher viability exceeding that of PEI(TA/PVPON)-coated cells for all combinations of components: for two and four bilayer shells and for different molecular weights of PVPON component. The highest viability was recorded for cells encapsulated with ultrathin two bilayer shells with the highest molecular weight of PVPON component, reaching 94% (Figure 7). The same shell with PEI pre-layer showed only 42%. For four bilayer shells, the viability slightly decreased to 85% but still remains much higher than that for shells with cationic PEI

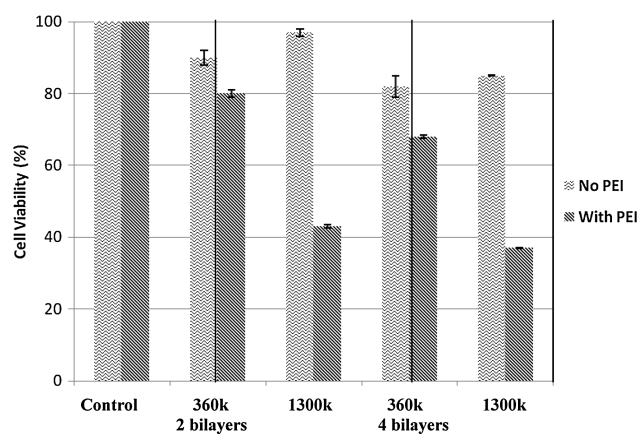


Figure 7. Viability (%) of yeast cells encapsulated with truly nonionic shells and shells with cationic component (2 and 4 bilayers) and the different molecular weights of PVPON component.

component. It is worth noting that higher molecular weight PVPON component promoted cell viability in the case of truly nonionic shells.

To estimate the permeability of low-molecular-weight reference molecules through shells, the diffusion of FITC across model (TA/PVPON) microcapsules was assessed, which emphasized significant difference in diffusion coefficients between true nonionic hydrogen-bonded and PEI-primed shells. To prepare such model microcapsules, shells were formed on sacrificial silica cores with diameters comparable to the cell dimensions. On the other hand, since basic nutrients (glucose, essential amino acids) and inducer molecules (galactose, $M_w = 180$ Da) are comparable in size with FITC molecules exploited here ($M_w = 380$ Da), we suggest that these molecules will also be able to freely diffuse through the shell and thus can serve for proper evaluation of molecular diffusion through these shells.

FITC diffusion was measured across shells with variable thickness by utilizing the well-known FRAP technique as described in detail elsewhere.^[39] Diffusion coefficient for nonionic (TA/PVPON) shells measured with this technique ranges from 1.5 to $5 \times 10^{-11} \text{ cm}^2 \cdot \text{s}^{-1}$ (Figure 8). Moreover, the diffusion coefficient gradually decreases with increasing the thickness of LbL shells. The values obtained here for any given shell thickness are close for all types of shells studied. However, PEI-containing shells obtained from lower concentration solution possess the highest diffusion coefficient for all compositions studied here (Figure 8).

These divergences can be associated with significant differences in shell morphologies as derived from AFM images (Figure 9a). The analysis of AFM images which allows for estimation of the shells thickness and surface microroughness reveals that the shell thickness increases consistently with the increasing of the number of layers: from 13 to 32 nm for different shell types. However, all LbL shells with cationic PEI component showed much higher thickness (by 30–50%) as compared to hydrogen-bonded TA/PVPON shells with shells assembled from lower

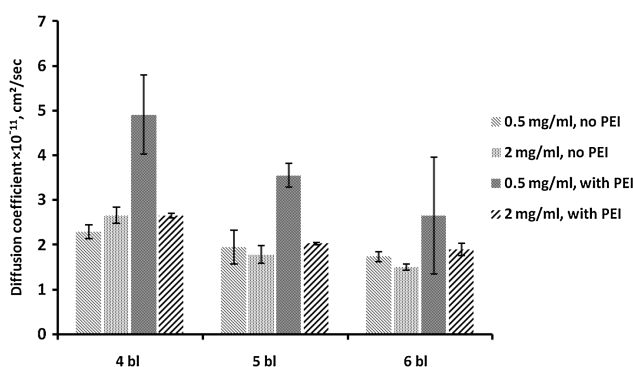


Figure 8. Diffusion coefficients of PEI(TA/PVPON) and (TA/PVPON) shells with different number of bilayers prepared from solutions with different concentrations.

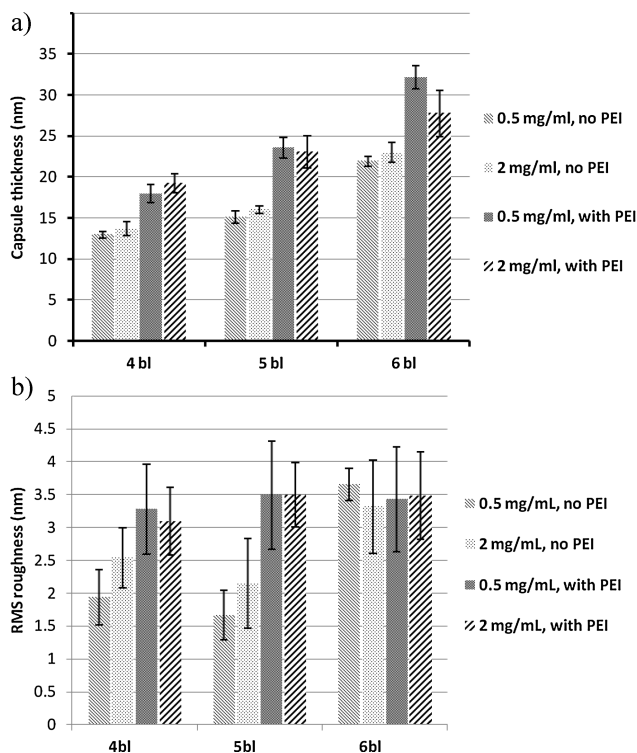


Figure 9. Thickness (a) and microroughness (b) of different types of LbL shells with different number of bilayers.

concentration solution usually being the highest. Shell surface microroughness is similar (around 3.5 nm) for all shell types with the highest number of bilayers studied here (Figure 9b). However, thinner shells without PEI pre-layer showed much smoother surfaces with microroughness close to 2 nm.

Based upon these results, we suggest how shell morphology affects the permeability properties. The schematic relates the highest permeability of thinnest LbL shells with PEI pre-layer to TA aggregation (Figure 10). TA has been shown to aggregate with its LbL counterpart (in this case, PEI

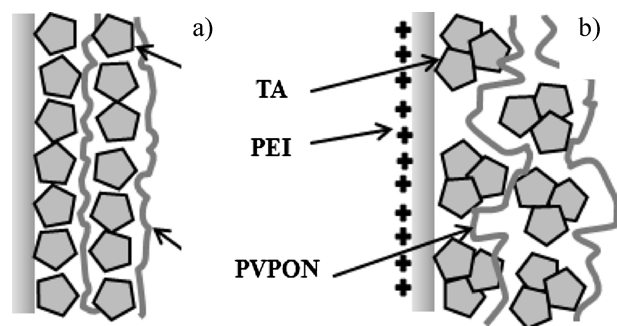


Figure 10. Fine morphology of (a) truly nonionic hydrogen-bonded shells, and (b) PEI-primed hydrogen-bonded shells. The positive charge of PEI-primed shells causes TA molecules to aggregate, resulting in thicker, and rougher shells.

or PVPON component) in hollow LbL shells.^[58,87] We suggest that this increased aggregation promoted by the presence of cationic chains causes significantly increased thickness and roughness of corresponding shells as well as gives rise to the loose, grainy morphology of PEI(TA/PVPON) shells noted previously.^[39] In contrast, the hydrogen bonds between layers of PEI-free shells produce thinner, more densely packed, and more uniform shells that facilitated a lower diffusion coefficient for (TA/PVPON) shells.

To further test the encapsulated cell ability to grow, we conducted continuous monitoring of their functioning. In fact, cells' ability to proliferate and express fluorescent component, yEGFP, after encapsulation can be taken indicative of preserved cell vital functions. In this test, yEGFP expression is induced by the addition of an initiating agent, galactose (Gal) to our *S. cerevisiae* yeast cells with incorporated yEGFP reporter.^[49,50,51]

The rate of yEGFP expression controls the rate of normalizing fluorescence variation of expressed yEGFP with strong green fluorescence (Figure 11). As apparent from this data, yEGFP is not generated in the absence of galactose. In contrast, initiated yeast cell growth displays a characteristic S-shaped curve with three phases: lag phase, exponential phase, and stationary phase.^[61] During the initial lag phase, cell division (growth rate) is slow in all cases, bare and encapsulated cells. This stage is followed by the exponential growth mode, where the cell division accelerates and a unicellular organism duplicates, i.e., one cell produces two in a given period of time. The exponential phase then proceeds to a stationary phase when there is no discernible change in cell concentration. Some reduction in fluorescence is caused by space and food limitation at a later stage. Very minute differences in curve shapes for bare and encapsulated cells with both three and four bilayers are indicative of negligible effect of the presence of the LbL shell on the cell expression function.

For comparative monitoring of cell growth in the absence and presence of cationic component, we further conducted

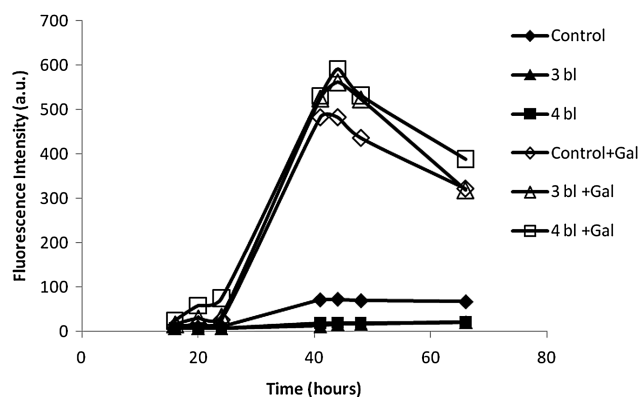


Figure 11. yEGFP expression of bare and encapsulated cells incubated with and without galactose.

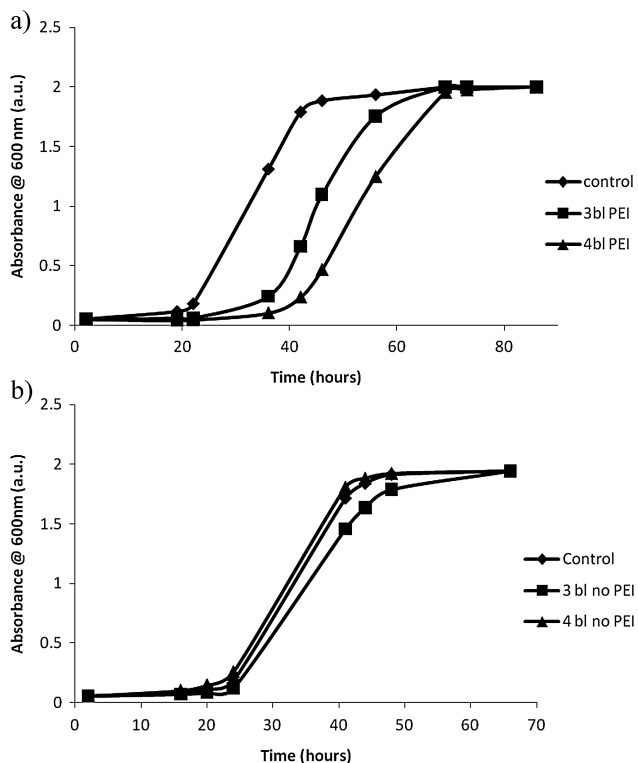


Figure 12. Characteristic S-shaped cell growth as measured by OD600. (a) Cells encapsulated with polycationic precursor PEI show significant delayed entrance into exponential phase, while (b) cells encapsulated with truly nonionic shells show no delay of cell growth.

concurrent optical density measurements of media containing (TA/PVPON)-coated cells and PEI-(TA/PVPON)-coated cells (Figure 12). Data for encapsulated cells were normalized using min-max normalization.^[88] As has been observed, a significant delay (up to 25 h) of the exponential phase for the PEI-(TA/PVPON)-coated cells depends on the thickness of the polymer coating with thicker shells resulting in large delay (Figure 12a).

In contrast, no significant delay (within uncertainty of 2–3 h) in cell growth has been observed for nonionic (TA/PVPON)-coated cells with different thicknesses (up to 13 nm) indicating insignificant interference of hydrogen-bonded shells with cell functioning and growth (Figure 12b). Considering that the permeability of fully nonionic shells is lower than that of cationic-containing shells this result might be considered surprising if one assumes that the exponential phase of growth is controlled by the rate of materials exchange across cell membrane. Thus, we suggest that the explanation for this apparent contradiction lies in the mechanical stability of the LbL shells and the fact that encapsulated cells actually begin to divide within the shell and further growth occurs by cells rupturing the shell.^[61] (TA/PVPON) shells with lower elastic

modulus (as will be discussed in a separate publication) are easily ruptured by dividing cells without much interference to their growth.

Conclusion

An enhanced strategy for cell encapsulation with LbL shells by exploiting truly nonionic hydrogen-bonded shells without use of any synthetic or natural polyelectrolyte components was reported. The elimination of the polycations as a traditional LbL pre-layer allows encapsulated cells to maintain a much higher viability (reaching 94%) as compared to cells encapsulated with the cationic pre-layer. It is worth noting the approach suggested here shows wide applicability. In fact, the preservation of very high viability observed immediately (few hours) after processing indicates minimal intrusion of hydrogen-bonding LbL assembly on cells and, on the other hand, minimal alteration in long-term (3 d) cell growth kinetics indicates insignificant effect on the nutrition supply, cell communication, and division.

This high cytocompatibility is a result of the cells having no exposure to cytotoxic polycations and from the high permeability of the shells. Additionally, the mechanical stability of the nonionic shells is such that the shell shape is maintained, but can be easily ruptured by dividing cells thus not interfering with the rate of cell growth in contrast to traditional polyelectrolyte shells. We expect that the fields of biomedical and biosensing sciences stand to benefit from such cell surface engineering utilizing non-cytotoxic, potentially stimulus-responsive LbL components.

Acknowledgements: This work was supported by the Air Force Office of Scientific Research FA9550-08-1-0446 and FA9550-09-1-0162 grants. The authors acknowledge Dr. Olga Shchepelina and Dr. Veronika Kozlovskaya for useful discussions and assistance.

Received: April 5, 2011; Revised: May 1, 2011; Published online: July 4, 2011; DOI: 10.1002/mabi.201100129

Keywords: atomic force microscopy (AFM); biological applications of polymers; cell encapsulation; layer-by-layer assembly; polymer membranes

- [1] Z. Tang, Y. Wang, P. Podsiadlo, N. A. Kotov, *Adv. Mater.* **2006**, *18*, 3203.
- [2] G. B. Sukhorukov, H. Möhwald, in *Colloids and Colloid Assemblies*, (Ed., F. Caruso), Wiley-VCH, Weinheim, Germany **2004**, p. 18.
- [3] I. Luzinov, S. Minko, V. V. Tsukruk, *Prog. Polym. Sci.* **2004**, *29*, 635.

- [4] M. C. Raymond, R. J. Neufeld, D. Poncelet, *Artif. Cells Blood Substit. Immobil. Biotechnol.* **2004**, *32*, 275.
- [5] J. T. Wilson, E. L. Chaikof, *Adv. Drug Delivery Rev.* **2008**, *60*, 124.
- [6] F. Caruso, D. Trau, H. Möhwald, R. Renneberg, *Langmuir* **2000**, *16*, 1485.
- [7] I. Gill, A. Ballesteros, *J. Am. Chem. Soc.* **1998**, *120*, 8587.
- [8] G. Carturan, R. Dal Toso, S. Boninsegna, R. Dal Monte, *J. Mater. Chem.* **2004**, *14*, 2087.
- [9] J. Bjerketorp, S. Hakansson, S. Belkin, J. K. Jansson, *Curr. Opin. Biotechnol.* **2006**, *17*, 43.
- [10] A. Coiffier, T. Coradin, C. Roux, O. M. M. Bouvet, J. Livage, *J. Mater. Chem.* **2001**, *11*, 2039.
- [11] D. Yu, J. Volponi, S. Chhabra, C. J. Brinker, A. Mulchandani, A. K. Singh, *Biosens. Bioelectron.* **2005**, *20*, 1433.
- [12] J. A. Rowley, G. Madlambayan, D. J. Mooney, *Biomaterials* **1999**, *20*, 45.
- [13] K. Smetana, Jr., *Biomaterials* **1993**, *14*, 1046.
- [14] E. Alsberg, H. J. Kong, Y. Hirano, M. K. Smith, A. Albeiruti, D. J. Mooney, *J. Dent. Res.* **2003**, *82*, 903.
- [15] A. D. Augst, H. J. Kong, D. J. Mooney, *Macromol. Biosci.* **2006**, *6*, 623.
- [16] G. Klock, A. Pfeffermann, C. Ryser, P. Grohn, B. Kuttler, H. J. Hahn, U. Zimmermann, *Biomaterials* **1997**, *18*, 707.
- [17] A. B. Lansdown, M. J. Payne, *J. R. Coll. Surg. Edinb.* **1994**, *39*, 284.
- [18] G. Decher, *Science* **1997**, *277*, 1232.
- [19] *Multilayer Thin Films*, (Eds., G. Decher, J. B. Schlenoff), Wiley-VCH, Weinheim, Germany **2003**.
- [20] *Protein Architecture: Interfacial Molecular Assembly and Immobilization Biotechnology*, (Eds., Y. Lvov, H. Möhwald), Marcel Dekker, New York **2000**.
- [21] Y. Lvov, G. Decher, H. Möhwald, *Langmuir* **1993**, *9*, 481.
- [22] C. Jiang, V. V. Tsukruk, *Adv. Mater.* **2006**, *18*, 829.
- [23] C. Jiang, V. V. Tsukruk, *Soft Matter* **2005**, *1*, 334.
- [24] A. A. Mamedov, N. A. Kotov, M. Prato, D. M. Guldi, J. P. Wicksted, A. Hirsch, *Nat. Mater.* **2002**, *1*, 190.
- [25] L. Zhai, A. J. Nolte, R. E. Cohen, M. F. Rubner, *Macromolecules* **2004**, *37*, 6113.
- [26] M. Nolte, B. Schoeler, C. S. Peyratout, D. G. Kurth, A. Fery, *Adv. Mater.* **2005**, *17*, 1665.
- [27] V. V. Tsukruk, F. Rinderspacher, V. N. Bliznyuk, *Langmuir* **1997**, *13*, 2171.
- [28] S. A. Sukhishvili, *Curr. Opin. Colloid Interface Sci.* **2005**, *10*, 37.
- [29] F. Caruso, *Adv. Mater.* **2001**, *13*, 11.
- [30] V. V. Tsukruk, V. N. Bliznyuk, D. W. Visser, A. L. Cambell, T. Bunning, W. W. Adams, *Macromolecules* **1997**, *30*, 6615.
- [31] J. D. Mendelsohn, C. J. Barrett, V. V. Chan, A. J. Pal, A. M. Mayes, M. F. Rubner, *Langmuir* **2000**, *16*, 5017.
- [32] A. Fery, B. Schöler, T. Cassagneau, F. Caruso, *Langmuir* **2001**, *17*, 3779.
- [33] K. Ariga, J. P. Hill, Q. Ji, *Macromol. Biosci.* **2008**, *8*, 981.
- [34] K. Ariga, Q. Ji, J. P. Hill, *Adv. Polym. Sci.* **2010**, *229*, 51.
- [35] C. Jiang, S. Markutsya, Y. Pikus, V. V. Tsukruk, *Nat. Mater.* **2004**, *3*, 721.
- [36] C. Jiang, S. Markutsya, H. Shulha, V. V. Tsukruk, *Adv. Mater.* **2005**, *17*, 1669.
- [37] D. Zimnitsky, C. Jiang, J. Xu, Z. Lin, L. Zhang, V. V. Tsukruk, *Langmuir* **2007**, *23*, 10176.
- [38] D. Zimnitsky, V. V. Shevchenko, V. V. Tsukruk, *Langmuir* **2008**, *24*, 5996.
- [39] H. Ko, C. Jiang, H. Shulha, V. V. Tsukruk, *Chem. Mater.* **2005**, *17*, 2490.
- [40] C. Jiang, S. Markutsya, H. Shulha, V. V. Tsukruk, *Adv. Mater.* **2005**, *17*, 1669.
- [41] P. T. Hammond, *Adv. Mater.* **2004**, *16*, 1271.
- [42] J. F. Quinn, A. P. R. Johnston, G. K. Such, A. N. Zelikin, F. Caruso, *Chem. Soc. Rev.* **2007**, *36*, 707.
- [43] L. L. del Mercato, P. Rivera-Gil, A. Z. Abbasi, M. Ochs, C. Ganas, I. Zins, C. Sonnichsen, W. J. Parak, *Nanoscale* **2010**, *2*, 458.
- [44] A. S. Hoffman, *Adv. Drug Delivery Rev.* **2002**, *54*, 3.
- [45] A. N. Zelikin, A. L. Becker, A. P. R. Johnston, K. L. Wark, F. Turatti, F. Caruso, *ACS Nano* **2007**, *1*, 63.
- [46] A. N. Zelikin, Q. Li, F. Caruso, *Chem. Mater.* **2008**, *20*, 2655.
- [47] V. Kozlovskaya, E. Kharlampieva, I. Erel, S. A. Sukhishvili, *Soft Matter* **2009**, *5*, 4077.
- [48] C. R. Kinnane, G. K. Such, G. Antequera-Garcia, Y. Yan, S. J. Dodds, L. M. Liz-Marzan, F. Caruso, *Biomacromolecules* **2009**, *10*, 2839.
- [49] B. Franz, F. Balkundi, C. Dahl, Y. Lvov, A. Prange, *Macromol. Biosci.* **2010**, *10*, 164.
- [50] S. Balkundi, M. Eby, G. Johnson, Y. Lvov, *Langmuir* **2009**, *25*, 14011.
- [51] H. Ai, M. Fang, S. Jones, Y. Lvov, *Biomacromolecules* **2002**, *3*, 560.
- [52] O. Shchepelina, V. Kozlovskaya, S. Singamaneni, E. Kharlampieva, V. V. Tsukruk, *J. Mater. Chem.* **2010**, *20*, 6587.
- [53] A. M. Shapiro, J. R. Lakey, E. A. Ryan, G. S. Korbutt, E. Toth, G. L. Warnock, N. M. Kneteman, R. V. Rajotte, *N. Engl. J. Med.* **2000**, *343*, 230.
- [54] F. Lim, A. M. Sun, *Science* **1980**, *210*, 908.
- [55] T. Bieber, W. Meissner, S. Kostin, A. Niemann, H. P. Elsasser, *J. Controlled Release* **2002**, *82*, 441.
- [56] W. T. Godbey, K. K. Wu, A. G. Mikos, *J. Biomed. Mater. Res.* **1999**, *45*, 268.
- [57] N. Veerabadran, S. Stewart, Y. Lvov, D. Mills, *Macromol. Biosci.* **2007**, *7*, 877.
- [58] J. F. Quinn, A. P. R. Johnston, G. K. Such, A. N. Zelikin, F. Caruso, *Chem. Soc. Rev.* **2007**, *36*, 707.
- [59] E. Kharlampieva, S. A. Sukhishvili, *Polym. Rev.* **2006**, *46*, 377.
- [60] E. Kharlampieva, V. Kozlovskaya, S. A. Sukhishvili, *Adv. Mater.* **2009**, *21*, 3053.
- [61] V. Kozlovskaya, S. Harbaugh, I. Drachuk, O. Shchepelina, N. Kelley-Loughnane, M. Stone, V. V. Tsukruk, *Soft Matter* **2011**, *7*, 2364.
- [62] I. Erel-Unal, S. A. Sukhishvili, *Macromolecules* **2008**, *41*, 3962.
- [63] D. M. Hushpalian, V. A. Fechina, S. V. Kazakov, I. Y. Sakharov, I. G. Gazaryan, *Biochemistry* **2003**, *68*, 1006.
- [64] J. Takebayashi, A. Tai, I. Yamamoto, *Biol. Pharm. Bull.* **2003**, *26*, 1368.
- [65] T. Shutova, V. Agabekov, Y. Lvov, *Russ. J. Gen. Chem.* **2007**, *77*, 1494.
- [66] V. Kozlovskaya, S. Yakovlev, M. Libera, S. A. Sukhishvili, *Macromolecules* **2005**, *38*, 4828.
- [67] G. J. M. Koper, R. C. van Duijvenbode, D. D. P. W. Stam, U. Steuierle, M. Borkovec, *Macromolecules* **2003**, *36*, 2500.
- [68] R. Mészáros, L. Thompson, M. Bos, P. de Groot, *Langmuir* **2002**, *18*, 6164.
- [69] C. Brunot, L. Ponsonnet, C. Lagneau, P. Farge, C. Picart, B. Grosgeat, *Biomaterials* **2007**, *28*, 632.
- [70] A. Goffeau, B. G. Barrell, H. Bussey, R. W. Davis, B. Dujon, H. Feldmann, F. Galibert, J. D. Hoheisel, C. Jacq, M. Johnston, E. J. Louis, H. W. Mewes, Y. Murakami, P. Philippsen, H. Tettelin, S. G. Oliver, *Science* **1996**, *274*, 546.
- [71] S. Shibusaki, M. Ueda, T. Iizuka, M. Hirayama, Y. Ikeda, N. Kamasawa, M. Osumi, A. Tanaka, *Appl. Microbiol. Biotechnol.* **2001**, *55*, 471.

- [72] R. Narayanaswamy, M. Levy, M. Tsechansky, G. M. Stovall, J. D. O'Connell, J. Mirrielees, A. D. Ellington, E. M. Marcotte, *Proc. Natl. Acad. Sci. USA* **2009**, *106*, 10147.
- [73] K. M. Slade, R. Baker, M. Chua, N. L. Thompson, G. J. Pielak, *Biochemistry* **2009**, *48*, 5083.
- [74] V. V. Tsukruk, D. H. Reneker, *Polymer* **1995**, *36*, 1791.
- [75] M. E. McConney, S. Singamaneni, V. V. Tsukruk, *Polym. Rev.* **2010**, *50*, 235.
- [76] G. Ibatrz, L. Dahne, E. Donath, H. Mohwald, *Chem. Mater.* **2002**, *14*, 4059.
- [77] K. Glinel, G. Sukhorukov, H. Mohwald, V. Khrenov, K. Tauer, *Macromol. Chem. Phys.* **2003**, *204*, 1784.
- [78] T. Zhang, L. Ge, H. Chi, *Bull. Chem. Soc. Jpn.* **2008**, *81*, 906.
- [79] V. Kozlovskaya, E. Kharlampieva, I. Drachuk, D. Cheng, V. V. Tsukruk, *Soft Matter* **2010**, *6*, 3596.
- [80] J. O'Brien, I. Wilson, T. Orton, F. Pognan, *Eur. J. Biochem./FEBS* **2000**, *267*, 5421.
- [81] B. J. Dutka, N. Nyholm, J. Petersen, *Water Res.* **1983**, *17*, 1363.
- [82] T. G. Shutava, S. S. Balkundi, P. Vangala, J. J. Steffan, R. L. Bigelow, J. A. Cardelli, D. P. O'Neal, Y. M. Lvov, *ACS Nano* **2009**, *3*, 1877.
- [83] K. M. Riedl, A. E. Hagerman, *J. Agric. Food Chem.* **2001**, *49*, 4917.
- [84] G. K. Lopes, H. M. Schulman, M. Hermes-Lima, *Biochim. Biophys. Acta* **1999**, *1472*, 142.
- [85] U. J. Strotmann, B. Butz, W. R. Bias, *Ecotoxicol. Environ. Saf.* **1993**, *25*, 79.
- [86] W. C. Mak, K. W. Sum, D. Trau, R. Renneberg, *IEE Proc. Nanobiotechnol.* **2004**, *151*, 67.
- [87] T. Shutava, M. Prouty, D. Kommireddy, Y. Lvov, *Macromolecules* **2005**, *38*, 2850.
- [88] A. Jain, K. Nandakumar, A. Ross, *Pattern Recognit.* **2005**, *38*, 2270.